SCALING OF FINE SCALE EDDIES IN TURBULENT CHANNEL FLOWS UP TO RE$_\tau$=800

M. Tanahashi, S.-J. Kang, T. Miyamoto, S. Shiokawa and T. Miyauchi
Department of Mechanical and Aerospace Engineering,
Tokyo Institute of Technology
2-12-1 Ookayama, Meguro-ku, Tokyo 152-8552, Japan
mtanahas@mes.titech.ac.jp, kang@navier.mes.titech.ac.jp, tmiyauch@mes.titech.ac.jp

ABSTRACT

To clarify the scaling law of fine scale eddies in turbulent channel flows, direct numerical simulations are conducted for Re_τ=180, 400 and 800. The diameter and the maximum azimuthal velocity of coherent fine eddies can be scaled by Kolmogorov micorscale (η) and Kolmogorov velocity (u_k). The most expected diameter and maximum azimuthal velocity are $8 \sim 10\eta$ and $1.2 \sim 2.0u_k$, respectively. Near the wall, the most expected diameter increases to 10η from 8η and the most expected maximum azimuthal velocity increases to $2.0u_k$ from $1.2u_k$. Strain rates at the center of the coherent fine scale eddies is small compared with the mean strain rate of the whole flow field. The strain rates acting on the fine scale eddies away from the wall coincide with those in homogeneous turbulence and turbulent mixing layer. However, relatively large strain rates are acting on the near-wall coherent fine scale eddies. The most expected angle between the intermediate eigen vector and the rotating axis of the fine scale eddy is about 15~17degrees, which is independent on the turbulent flow fields. The probability that coherent fine scale eddies exist in low-speed streaks is higher than that in high-speed streaks. Large scale structures of wall turbulence are visualized by showing spatial distributions of central axes of coherent fine scale eddies.

INTRODUCTION

Theoretical description of intermittent character in small scale motion have been one of the most important subjects in turbulence research. Theorists have made efforts to establish a theory of fine scale structure of turbulence by assuming various type of vortices as fine scale structure (Townsend, 1951; Corrsin, 1962; Tennekes, 1968; Lundgren, 1982; Pullin et al., 1993). Most of them are based on an assumption that many tube-like vortices are embedded in turbulence randomly. Owing to direct numerical simulations (DNS) of turbulence, it has been found that turbulence is composed of universal fine scale eddies, which are verified in homogeneous isotropic turbulence (Jimenez et al., 1993; Tanahashi et al., 1999a), turbulent mixing layer (Tanahashi et al., 2001) and turbulent channel flow (Tanahashi et al., 1999c). In turbulent mixing layers, large scale structures which were found by Brown & Roshoko (1974) are composed of coherent fine scale eddies (Tanahashi et al., 2001). In turbulent channel flows, well-known streamwise vortices possess the same feature as the coherent fine scale eddies (Tanahashi et al., 1999b, 1999c). The characteristics of these eddies in low Reynolds number flows can be scaled by the Kolmogorov micro scale (η) and r.m.s. of velocity fluctuation (u_{rms}), and the most expected diameter and maximum azimuthal velocity are about 8η and 0.5~1.0 u_{rms}, respectively. Recent study in homogeneous isotropic turbulence up to $Re_\lambda \approx 220$ have revealed the exact scaling of these coherent fine scale eddies (Miyauchi et al., 2002). The diameter and the maximum azimuthal velocity are scaled by η and the Kolmogorov velocity (u_k), respectively. Similar to the results obtained in low Re_λ cases (Jimenez et al., 1993; Tanahashi et al., 1999a), the most expected diameter is 8η even for highest Re_λ. On the other hand, the most expected value of the maximum azimuthal velocity can be scaled by u_k instead of u_{rms} and is $1.2u_k$ for all Re_λ. It should be noted that the azimuthal velocity of intense fine scale eddies of which diameter is about 8η remains to be scaled by u_{rms} and reaches to $3 \sim 4$ u_{rms} even at high Re_λ.

From previous studies for homogeneous isotropic turbulence and turbulent mixing layer, it has been reported that the most expected eigen value ratio is -5:1:4, and the eigen vectors of the minimum eigen value tends to be perpendicular to the rotating axis of the coherent fine scale eddy and the angle between the rotating axis and the eigen vector of intermediate eigen value is less than 45 degrees for about 70 percents of the fine scale eddy (Tanahashi et al., 2001; Miyauchi et al., 2002). Blackburn et al. (1996) have reported that the eigen vector of the intermediate eigen value shows a tendency to be parallel with vorticiy vector in the near-wall of turbulent channel flow with Re_τ=395. Tanahashi et al. (1999c) have investigated the alignment and the ratio of the eigen values at the center of coherent fine scale eddy for low Reynolds number cases.

Over the past few decades, a number of studies have been conducted on relation between a low-speed streaks and the structure of wall turbulence. The average length of a low-speed streak associated with a hairpin vortex is about two to three hundred wall units in low-Reynolds number channel flow (Kim, 1983). The most widely observed coherent structures in the wall layer are streaks: elongated regions of high- and low-speed fluid alternating in the spanwise direction (Choi et al., 1994). The generation of the quasi-streamwise vortices is associated with changes in the shape of a low-speed streak surface (Soldati, 2000). However, there are few studies about quantitative relations between low-speed streaks and coherent fine scale eddies. For identification of vortical structures in turbulent flow, a considerable number of investigations have been reported. For example, Tanaka et al. (1993) have used $\nabla^2 p$ to represent streamwise vortices in homogenous shear flows. $\nabla^2 p$ corresponds to two times of second invariant Q of velocity gradient tensor. Jeong et al. (1997) and Blackborn et al. (1996) have used λ_2 definition and Δ definition to investigate vortical structure near the wall. However, all of these identification methods depend on the threshold of the variable.

In this study, direct numerical simulations of turbulent

Table 1: Numerical parameters for DNS of turbulent channel flows.

Re_τ	Re	$L_x \times L_y \times L_z$	$N_x \times N_y \times N_z$
180	3276	$4\pi\delta \times 2\delta \times \pi\delta$	192×193×160
400	8200	$2\pi\delta \times \delta \times \pi\delta$	256×385×192
800	17760	$2\pi\delta \times \delta \times \pi\delta$	512×769×384

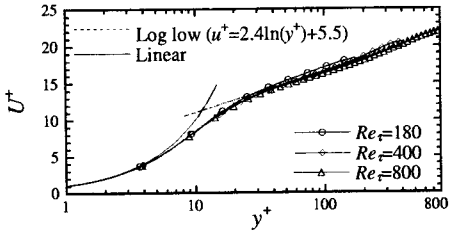

Figure 1: Mean velocity profiles for Re_τ=180, 400 and 800.

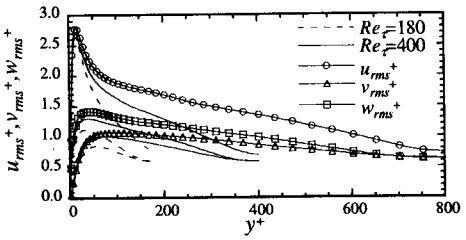

Figure 2: Root-mean-square velocity fluctuations for Re_τ=180, 400 and 800.

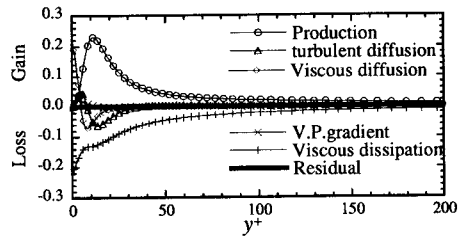

Figure 3: The budget of the transport equation for the turbulent energy (Re_τ=800).

channel flow up to Re_τ=800 are conducted. From these DNS data, the scaling law of fine scale eddies near the wall is investigated, and large and small scale coherent structures of wall turbulence are visualized by showing spatial distributions of the axes of coherent fine scale eddies.

TURBULENT STATISTICS

In this study, direct numerical simulations of turbulent channel flows up to Re_τ=800 were conducted by solving incompressible Navier-Stokes equations and continuity equation. The parameters of direct numerical simulation for turbulent channel flows are given in Table 1. Spectral methods are used in the streamwise (x) and spanwise (z) directions, and 4th-order central finite difference scheme is used in the transverse (y) direction. This DNS code has been verified by comparing with the result of Kim et al. (1987). Computations were carried out until turbulent flow field attains statistical steady state.

Figure 1 shows the mean velocity profiles for Re_τ=180, 400 and 800, where the wall-normal coordinate is given in wall units and the mean velocity is normalized by the friction velocity (u_τ). The solid and dashed lines represent the linear and the log laws, respectively. The all curves in $y^+ < 5$

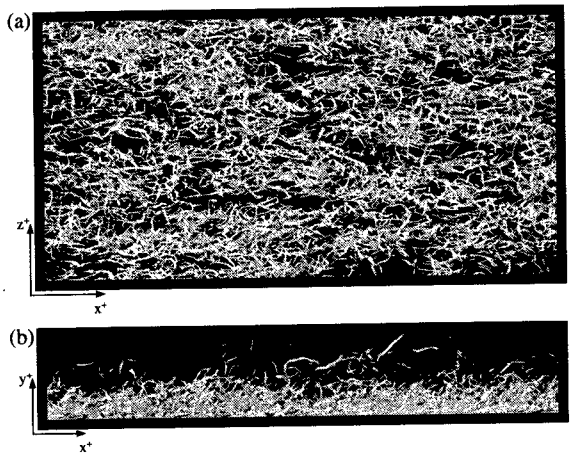

Figure 4: Iso-surfaces of the second invariant of the velocity gradient tensor for Re_τ=800 (Q=10, domain size: $l_x^+ \times l_y^+ \times l_z^+ = 5026 \times 800 \times 2513$). (a) top view, (b) side view.

are independent on Re_τ. The curves in $y^+ > 20$ both for Re_τ=400 and 800 coincide with the dashed line, but the curve of Re_τ=180 shifts upward from it. Moreover, it should be noted that the wake region is clearly distinguishable for Re_τ=800. Root-mean-square velocity fluctuations normalized by u_τ are shown in Fig. 2. These peak values slightly increase with the increase of Re_τ. Especially, wall-normal and spanwise components highly depend on Re_τ and positions of the peak values are slightly away from the wall as Re_τ is increased.

Figure 3 shows the budget of the turbulent kinetic energy for Re_τ=800 in wall coordinates. The absolute values of the production and the dissipation terms are larger than the results for Re_τ=180 and 400, but the ratio of these terms is independent on Re_τ as shown by Moser et al. (1999). We could verify that the budget of the transport equation for the Reynolds stress also shows the similar trend with the budget of the turbulent kinetic energy and these residuals are almost zero.

FINE SCALE EDDIES OF HIGH REYNOLDS NUMBER TURBULENT CHANNEL FLOW

There are a lot of methods for identification of vortical structures in turbulent flows. High vorticity or enstrophy regions are the simplest method to visualize the vortical structures. In previous works related to fine scale structures in homogeneous isotropic turbulence, high vorticity regions have been used to identify the intermittent fine scale structure of turbulence (Jimenez et al., 1993; She et al., 1990). However, high vorticity regions may represent tube-like and sheet-like structures simultaneously. For the case with a strong mean shear like the flows near wall or center of free shear flows, employment of high vorticity or enstrophy regions fails to represent coherent eddies. For visualization purpose, iso-surfaces of the second invariant of the velocity gradient tensor are shown for Re_τ=800 in Fig. 4. The region visualized is the lower half of calculation domain. The second invariant of the velocity gradient tensor is given by $Q(=(W_{ij}W_{ij} - S_{ij}S_{ij})/2)$, where $S_{ij}(=(\partial u_i/\partial x_j + \partial u_j/\partial x_i)/2)$ and $W_{ij}(=(\partial u_i/\partial x_j - \partial u_j/\partial x_i)/2)$ are the symmetric and asymmetric parts of the velocity gradient tensor $A_{ij}(=\partial u_i/\partial x_j = S_{ij}+W_{ij})$. Figure 4 indicates that there are a lot of tube-like structures in turbulent channel flow same as in homogeneous isotropic turbulence and turbulent mixing layer. In turbulent channel flow, stream-

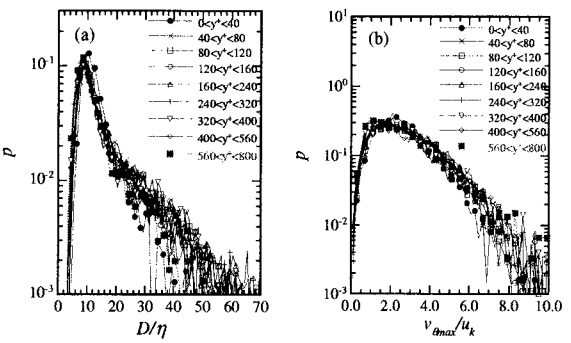

Figure 5: Probability density functions of diameter (a) and azimuthal velocity (b) of the coherent fine scale eddies for Re_τ=800.

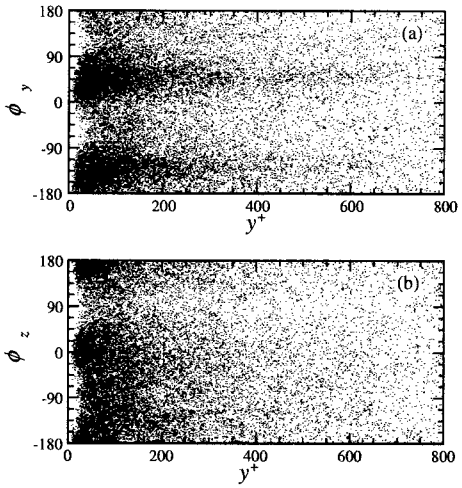

Figure 6: The inclination angle (a) and the tilting angle (b) of the coherent fine scale eddies (Re_τ =800).

wise vortices near the wall and hairpin-like vortices can be visualized by the positive Q region. Jeong et al. (1997) and Blackborn et al. (1996) have used λ_2 definition and Δ definition to investigate vortical structure near the wall. However, all of the visualization including Fig. 4 depend on the threshold of the variable. Therefore, in this study, fine scale eddies are educed without any threshold by using new identification scheme based on local flow pattern which was used in our previous studies on homogeneous isotropic turbulence (Tanahashi et al., 1999a). From the distribution of Q, two-dimensional sections of fine scale eddies are identified by using the new identification scheme. The educed section includes a local maximum of Q along the axis of a fine scale eddy and a center point of swirling motion is identified. Figure 5 shows the probability density functions (pdf) of the diameter and the maximum azimuthal velocity of the fine scale eddies for Re_τ=800. The diameter and the maximum azimuthal velocity are normalized by η and u_k, which are calculated from mean energy dissipation rate at y^+ where the eddy exists. The both pdfs do not depend on Re_τ (the results for low Re_τ cases are not shown here), whereas they have weak y^+-dependence. Near the wall, the most expected diameter and maximum azimuthal velocity are about 10η and $2.0u_k$, respectively. Leaving from the wall, the most expected diameter and maximum azimuthal velocity become about 8η and $1.2u_k$, which coincides with those in homogeneous isotropic turbulence (Miyauchi et al., 2002). The fine scale eddies near the wall such as the streamwise vortices and hairpin-like vortices are slightly wider and

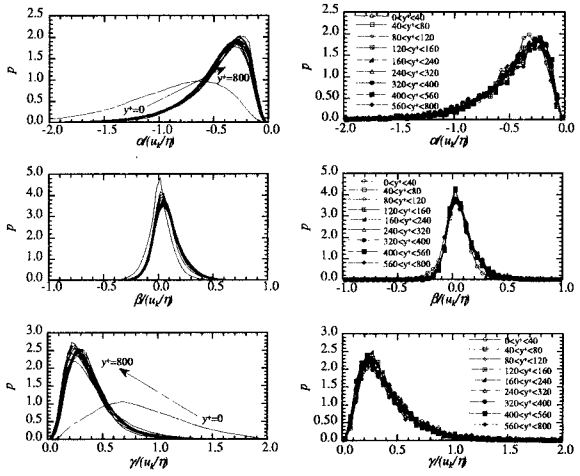

(a) (b)

Figure 7: Probability density functions of eigen values of the strain tensor for Re_τ=800. (a) whole flow field (every 20 y^+), (b) at the center of coherent fine scale eddies.

stronger than those in homogeneous isotropic turbulence.

In addition to the diameter and the maximum azimuthal velocity, the spatial distribution of the axes also shows characteristic feature near the wall. Figure 6 shows the inclination angles and the tilting angles of the coherent fine scale eddies for Re_τ=800. The inclination angle and the tilting angle are defined by the similar method of Jeong et al. (1997). These two angles show strong directional dependence with the decrease of y^+. These features correspond to hairpin-like eddies and streamwise vortices observed near the wall (Tanahashi et al., 1999b, 1999c). Figure 6 suggests that directional dependence of the axis can be observed even for $y^+ \approx 600$. The variance of the diameters becomes relatively small near the wall as shown in Fig. 5(a), and diameter of almost all coherent fine scale eddies near the wall is about 10η. Therefore, the anisotropy near the wall can be attributed to the smallest coherent fine scale eddies. These results suggest that the anisotropic feature in near-wall turbulence is significantly different from that in free-shear turbulence (Tanahashi et al., 2001) from the viewpoint of the fine scale structure.

COHERENT FINE SCALE EDDY AND STRAIN FIELD

Strain rate acting on the coherent fine scale eddies is investigated by evaluating the strain rate tensor S_{ij} at the center of the coherent fine scale eddies. The definitions of eigen values and eigen vectors of S_{ij} are given by

$$\boldsymbol{S} = \boldsymbol{R}\begin{pmatrix} \alpha & 0 & 0 \\ 0 & \beta & 0 \\ 0 & 0 & \gamma \end{pmatrix}\boldsymbol{R}^T,\ \boldsymbol{R} = \left(e_\alpha, e_\beta, e_\gamma\right), \quad (1)$$

where α, β and γ are the minimum, intermediate and maximum eigen values respectively. The unit eigen vectors corresponding to α, β and γ are represented by e_α, e_β and e_γ. Due to the assumption of incompressibility, these can be expressed by the relational equation of $\alpha+\beta+\gamma=0\,(\alpha \le 0 \le \gamma,\ \alpha \le \beta)$. θ, ψ and ϕ are defined by the angles between the rotating axes of coherent fine scale eddies (vorticity vector $\boldsymbol{\omega}$ at the center of coherent fine scale eddies) and three unit eigen vectors e_α, e_β and e_γ.

Figure 7 (a) shows pdfs of the eigen values at the whole flow field. The eigen values are normalized by η and u_k. Near the wall, the pdf of intermediate eigen value indicates

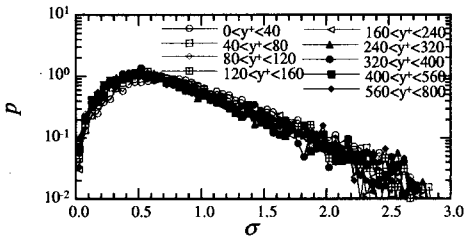

Figure 8: Probability density functions of eigen value ratio at the center of coherent fine scale eddies (Re_τ=800).

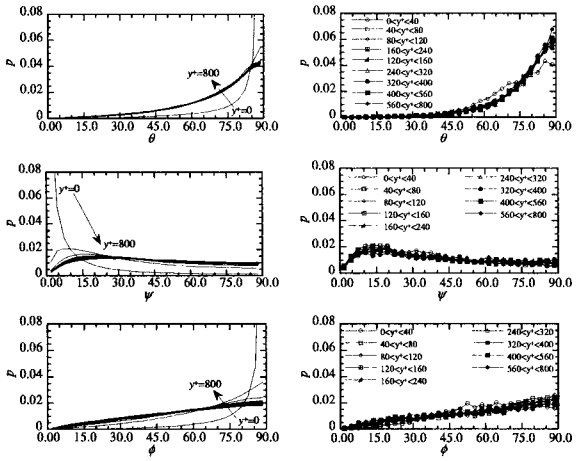

(a) (b)

Figure 9: Probability density functions of the angles between unit eigen vectors of strain rate tensor and vorticity vectors for Re_τ=800. (a) whole flow field, (b) at the center of coherent fine scale eddies.

a sharp peak at about zero, but it skews into the positive portion and the most expected value becomes about $0.06u_k/\eta$ far from the wall. The most expected minimum eigen value increases with the increase of distance from the wall, while the most expected maximum eigen value decreases. Figure 7(b) shows pdfs of the eigen values evaluated at centers of the coherent fine scale eddies. The eigen values in Fig. 7(b) are also normalized by u_k/η as in Fig. 7(a). Pdfs of the eigen values near the wall are different from those at the channel center. Near the wall, pdfs of α, β and γ show peaks at about -0.32, 0.04 and 0.27 u_k/η, respectively. At the center of channel, these peak values are -0.25, 0.04 and 0.02 u_k/η respectively, which coincides with the cases of homogeneous isotropic turbulence and turbulent mixing layer. Pdfs of the eigen values of strain rate acting on the center of coherent fine scale eddies show a very good agreement with those obtained from the whole flow field except for the near-wall region, but the absolute values of the most expected eigen values are smaller than those obtained from the whole flow field. In other words, these results suggest that strain rate acting on the center of coherent fine scale eddies is smaller than that in the mean shear field.

To investigate the ratio of eigen values at centers of the coherent fine scale eddies, an eigen value ratio σ is introduced by $\sigma = (\gamma - \beta)/(\gamma + \beta)$ $(0 \leq \sigma \leq 3)$. Figure 8 shows the pdf of the eigen value ratio for Re_τ= 800. The peak of pdf increases from about 0.6 to 0.7 near the wall. The most expected eigen value ratio corresponding to σ = 0.6 is α:β:γ = -5:1:4 from the incompressible constraint. This eigen value ratio coincides with that in homogeneous isotropic turbulence and turbulent mixing layer (Tanahashi et al., 2001). Since the eigen value ratio shows a peak at σ = 0.7 near

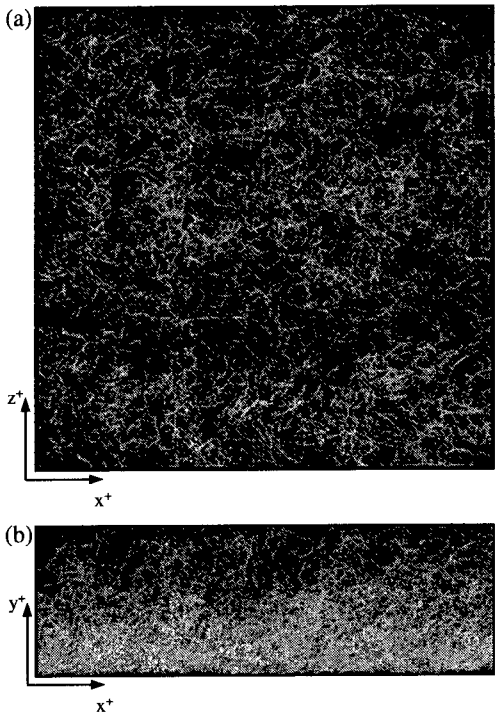

Figure 10: Spatial distributions of central axes of the coherent fine scale eddies for Re_τ=800 (domain size: $l_x^+ \times l_y^+ \times l_z^+$ = 2513 × 800 × 2513). (a) top view, (b) side view.

the wall, the most expected eigen value ratio becomes α:β:γ = -7:1:6. Note that the large compression and stretching are acting on the coherent fine scale eddies in the near-wall region. Figure 9(a) shows pdfs of the angles between the local vorticity vectors and the unit eigen vectors of strain rate in the whole flow field. Near the wall, probabilities of θ, ψ and ϕ show peaks at θ = 90, ψ = 0 and ϕ = 90, respectively. Far from the wall, pdfs of ψ show peak at about 25 degree, but those of θ and ϕ still do peak at about 90 degrees. Pdfs of the angles between the unit eigen vectors and the axes of coherent fine scale eddies are plotted in Fig. 9(b). Pdfs of θ and ϕ show similar trends with those in Fig. 9(a) except for the region near the wall, but probabilities near the peaks at about 90 degrees are higher than those in the whole flow field. The probability of peak for ψ in the near-wall region is lower than that in the channel center. In the near-wall region, pdf of ψ sharply increases from zero and gradually decreases after showing peaks at about 15∼17 degrees. These results reveal that the rotating axes of the coherent fine scale eddies are perpendicular to the eigen vectors of the minimum and maximum eigen values, and the eddies receive the strong compression and stretching in that direction. The most of coherent fine scale eddies receive a weak stretching corresponding to the intermediate eigen value with the misalignment of about 15∼17 degrees with respect to the axial direction of the fine scale eddies. These features do not depend on Reynolds number.

SPATIAL DISTRIBUTIONS OF CENTRAL AXES OF THE COHERENT FINE SCALE EDDIES

To investigate spatial distribution of the coherent fine scale eddies, the central axes of the fine scale eddies were identified by using axis tracing method (Tanahashi et al., 1999d). Figure 10 shows spatial distributions of central axes of the coherent fine scale eddies for Re_τ=800. The visualization in Fig. 10 includes all vortical structures because the

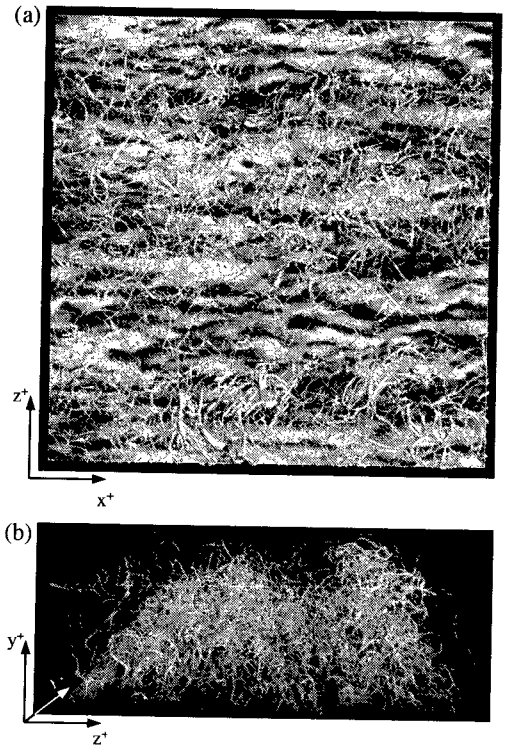

Figure 11: Spatial distributions of central axes of the coherent fine scale eddies with contour of the instantaneous streamwise velocity fluctuation at y^+=20 for Re_τ=800 (domain size: $l_x^+ \times l_y^+ \times l_z^+ = 2513 \times 800 \times 2513$). Diameter of axis was drawn to be proportional with $\sqrt{Q^*}$. (a) top view, (b) perspective view from the upstream.

axis, which specify the positions in space, is independent to the threshold of variables. Spatial distributions of the axes in Fig. 10 show that the coherent fine eddies exist not only in the near-wall region but also in the whole flow field. Moreover, it is worth noting that central axes of the coherent fine scale eddies are distributed in viscous sub-layer for all three Re_τ cases, and axis positions nearest to the wall are about y^+=0.6, 0.8 and 0.9 for Re_τ=180, 400 and 800, respectively.

Figure 11 shows spatial distributions of the axes of the coherent fine scale eddies with contour of the instantaneous streamwise velocity at y^+= 20 for Re_τ=800. In contour of the streamwise velocity, light-gray and dark-gray indicate high- and low-speed regions, respectively. Diameter of a central axis was drawn to be proportional with $\sqrt{Q^*}$ on the axes and Q^* is normalized by η and u_k. Therefore, wider axes possess stronger rotation rate. It is observed that the large clusters of central axes of the coherent fine scale eddies appear with a spanwise spacing of about 1100~1200 wall units. To deeply inspect relation between the axes of the coherent fine scale eddies and high- and low-speed regions in Fig. 11, detailed spatial distributions are shown in Fig. 12 as a function of y^+. In Fig. 12(a), it is clearly observed that central axes in low-speed streaks possess the relatively stronger rotation rate near the wall. The distributions with the weaker rotation rate are not so related with low-speed streaks. Above tendencies are hardly dependent on the wall-normal direction, but the lateral spacing between low-speed regions becomes wider leaving from the wall as shown in Fig. 12(b). These results suggest that low-speed streaks possess relatively larger second invariant of the velocity gradient tensor, which is closely related with fine scale eddies possessing the stronger rotation rate.

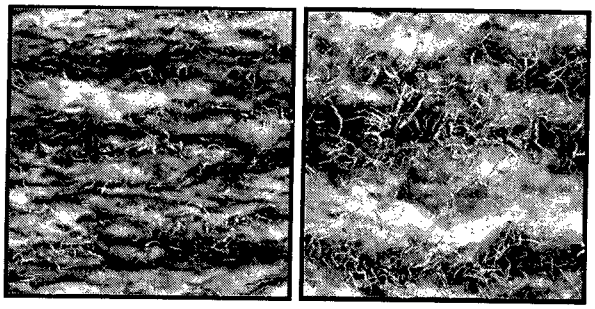

(a) (b)

Figure 12: The y^+ dependence of the axis distribution of the coherent fine scale eddies (Re_τ = 800, top view, domain size: $l_x^+ \times l_z^+ = 2513 \times 2513$). (a) $l_y^+ = 39 \sim 60$, u'^+ contour at $y^+ = 40$, (b) $l_y^+ = 199 \sim 400$, u'^+ contour at $y^+ = 200$.

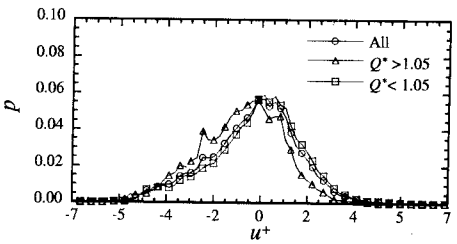

Figure 13: The probability density function of the instantaneous streamwise velocity on the central axes of the coherent fine scale eddies (Re_τ=800).

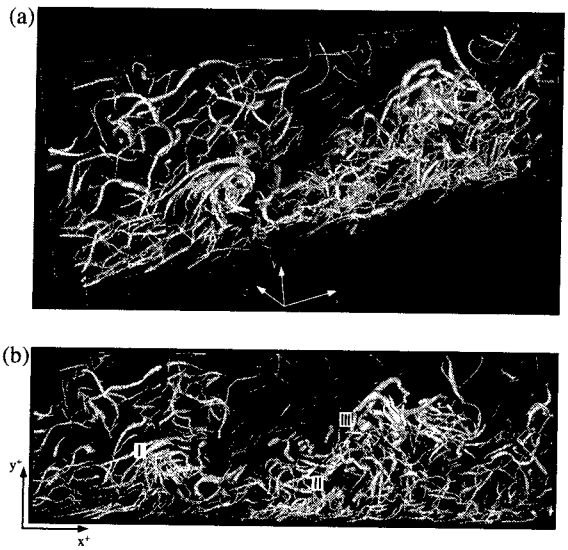

Figure 14: Spatial distributions of central axes of the coherent fine scale eddies for Re_τ=800. Diameter of axis was drawn to be proportional with $\sqrt{Q^*}$ (domain size: $l_x^+ \times l_y^+ \times l_z^+ = 2513 \times 800 \times 328$). (a) perspective view from above and upstream, (b) side view.

To estimate relation between the streak structure and the rotation rate of the coherent fine scale eddies quantitatively, conditioned pdfs of the instantaneous streamwise velocity on the central axes of the coherent fine scale eddies is plotted in Fig. 13. The triangle and the rectangle symbols indicate pdfs conditioned by $Q^* > 1.05$ and $Q^* < 1.05$, respectively. For comparison, pdf of u'^+ without the condition is plotted. Here, the Q^* is the average value of Q^* at central axes of the coherent fine scale eddies, and Q^* is normalized by η and u_k. The pdf of u'^+ for $Q^* > 1.05$ indicates that the probability in the low-speed regions is higher than that in the high-speed regions. The percentages of axis in the low-

speed regions are 53.5% for all axes, 66.0% for $Q^* > 1.05$ and 48.7% for $Q^* < 1.05$.

To investigate structures of the fine scale eddies in details, spatial distributions of central axes in a typical domain are magnified in Fig. 14. The visualized region is x^+=0$\sim$2513, y^+=0$\sim$800 and z^+= 785 $\sim$ 1113, and the visualization method are the same in Fig. 11. It is clearly observed that hairpin-like eddies and their packets (Adrian et al., 2000) exist in labeled zones I, II and III. Moreover, the two large clusters involving the pockets of hairpin-like vortices are extended like mountains in the streamwise direction (see II and III regions). The hairpin-like vortices are one kinds of the coherent fine scale eddies, and their clusters or packets make further larger clusters of eddies.

CONCLUSIONS

In the present study, DNS of turbulent channel flow was carried out up to Re_τ= 800 to investigate scaling law of fine scale eddies and their spatial distribution. To educe fine scale eddies without any threshold, a new identification scheme based on local flow pattern was employed. The detected coherent fine scale eddies in turbulent channel flow can be scaled by the Kolomogorov microscale and the Kolomogorov velocity. In the near-wall region, the most expected diameter and maximum azimuthal velocity are about 10 times of the Kolomogorov microscale and 2.0 times of the Kolomogorov velocity, but become about 8 times of the Kolomogorov microscale and 1.2 times of the Kolomogorov velocity leaving from the wall. These results do not depend on Reynolds number. Spatial distributions of the rotating axes of fine scale eddies show characteristic feature near the wall. The directional dependence of the axis is observed even for $y^+ \approx 600$. Strain rate acting on the coherent fine scale eddies can be scaled by the Kolomogorov microscale and the Kolomogorov velocity. The most expected eigen value ratio is α:β:γ = -7:1:6 near the wall, but it becomes α:β:γ = -5:1:4 leaving from the wall. It is indicated that the large compression and stretching are acing on the rotating plane of the coherent fine scale eddies near the wall. The eigen vector of the minimum eigen value has a tendency to be perpendicular to the axis of the coherent fine scale eddy and the most expected angles between the axis and eigen vector of the intermediate eigen value are about 15$\sim$17 degrees.

Central axes of the coherent fine scale eddies are distributed even in the viscous sub-layer. They form the large clusters with a spanwise spacing of about 1100$\sim$1200 wall units far from the wall ($y^+ \approx 400$). Relation between the instantaneous streamwise velocity and central axes shows that the stronger coherent fine scale eddies tend to exist in low-speed regions. Spatial distributions of central axes also show that hairpin-like vortices are one feature of the coherent fine scale eddies. In addition, the packets of hairpin-like vortices can form further larger clusters of eddies.

REFERENCES

Adrian, R.J., Meinhart, C.D., and Tomkins, C.D., 2000, "Vortex organization in the outer region of the turbulent boundary layer", *J. Fluid Mech.*, Vol. 422, pp. 1-54.

Blackburn, H.M., Mansour, N.N., and Cantwell, B.J., 1996, "Topology of fine-scale motions in turbulent channel flow", *J. Fluid Mech.*, Vol. 310, pp. 269-292.

Brown, G.L., and Roshko, A., 1974, "On density effects and large structure in turbulent mixing layers", *J. Fluid Mech.*, Vol. 64, pp. 775-816.

Choi, H., Moin, P. and Kim, J., 1994, "Active turbulence control for drag reduction in wall-bounded flows", *J. Fluid Mech.*, Vol. 262, pp. 75-110.

Corrsin, S., 1962, "Turbulent dissipation fluctuations", *Phys. Fluids*, Vol. 10, pp. 1301-1302.

Jeong, J., Hussain, F., Schoppa, W., and Kim, J., 1997, "Coherent structures near the wall in a turbulent channel flow", *J. Fluid Mech.*, Vol. 332, pp. 185-214.

Jimenez, J., Wray, A.A., Saffman, P.G., and Rogallo, R.S., 1993, "The structure of intense vorticity in isotropic turbulence", *J. Fluid Mech.*, Vol. 255, pp. 65-90.

Kim, J., Moin, P., and Moser, R.D., 1987, "Turbulence statistics in fully developed channel flow at low Reynolds number", *J. Fluid Mech.*, Vol. 177, pp. 133-166.

Kim, J., 1983, "On the structure of wall-bounded turbulent flows", *Phys. Fluids*, Vol. 26, pp.2088-2097.

Lundgren, T.S., 1982, "Strained spiral vortex model for turbulent fine structure", *Phys. Fluids*, Vol. 25, pp. 2193-2203.

Moser, R.D., Kim, J., and Mansour, N.N., 1999, "Direct numerical simulation of turbulent channel flow up to Re_τ=590", *Phys. Fluids*, Vol. 11, pp. 943-945.

Miyauchi, T., Tanahashi, M., and Iwase, S., 2002, "Coherent fine scale eddies and energy dissipation rate in homogeneous isotropic turbulence up to $Re_\lambda \approx 220$", *presented at IUTAM symposium on high Reynolds number turbulence.*

Pullin, D.I., and Saffiman, P.G., 1993, "On the Lundgren-Townsend model of turbulent fine scales", *Phys. Fluids*, Vol. A5, pp. 126-145.

She, Z.S., Jackson, E. and Orszag, S.A., 1990, "Intermittent vortex structures in homogeneous isotropic turbulence", *Nature*, Vol. 344, pp.226-228.

Soldati, A., 2000, "Modulation of turbulent boundary layer by EHD flows", *ERCOFTAC Bulletin*, Vol. 44, pp. 50-56.

Townsend, A.A., 1951, "On the fine-scale structure of turbulence", *Proc., R. Soc.*, London, A208, pp. 534-542.

Tennekes, H., 1968, "Simple model for the small-scale structure of turbulence", *Phys. Fluids*, Vol. 11, pp. 669-761.

Tanahashi, M., Iwase, S., and Miyauchi, T., 2001, "Appearance and alignment with strain rate of coherent fine scale eddies in turbulent mixing layer", *Journal of Turbulence*, Vol. 2, No.6.

Tanahashi, M., Miyauchi, T., and Ikeda, J., 1999a, "Identification of coherent fine scale structure in turbulence", *Simulation and Identification of Organized Structures in Flow*, pp. 131-140

Tanahashi, M., Das, S.K., Shoji, K., and Miyauchi, T., 1999b, "Coherent fine scale structures in turbulent channel flows", *Trans. JSME*, Vol. 65, pp. 3244-3251.

Tanahashi, M., Shiokawa, S., Das, S.K., and Miyauchi, T., 1999c, "Scaling of fine scale eddies in near-wall turbulence", *J. Jpn. Soc. Fluid Mech.*, Vol. 18, pp. 256-261.

Tanahashi, M., Iwase, S., Uddin, Md.A., and Miyauchi T., 1999d, "Three-dimensioinal features of coherent fine scale eddies in turbulence", *Proc., 1st Int. Symp. Turbulence and Shear Flow Phenomena*, Begell House Inc., pp. 79-84.

Tanaka, M., and Kida, S., 1993, "Characterization of vortex tubes and sheets", *Phys. Fluids*, Vol. A5, pp. 2079-2082.

Zhou, J., Adrian, R.J., Balachandar, S., and Kendall, T.M., 1999, "Mechanisms for generating coherent packets of hairpin vortices in channel flow", *J. Fluid Mech.*, Vol. 387, pp. 353-396.